

Differential functional consequences of *GRIN2A* mutations associated with schizophrenia and neurodevelopmental disorders

Nate Shepard¹, David Baez-Nieto¹, Sumaiya Iqbal², Erkin Kurganov¹, Nikita Budnik¹, Arthur J. Campbell¹, Jen Q Pan¹, Morgan Sheng^{1,3*}, Zohreh Farsi^{1*}

¹Stanley Center for Psychiatric Research, Broad Institute of MIT and Harvard, Cambridge, MA, USA

²The Center for the Development of Therapeutics, Broad Institute of MIT and Harvard, Cambridge, MA, USA

³Department of Brain and Cognitive Sciences, Massachusetts Institute of Technology, Cambridge, MA, USA

*Correspondence: msheng@broadinstitute.org and zfarsi@broadinstitute.org.

Figure S1

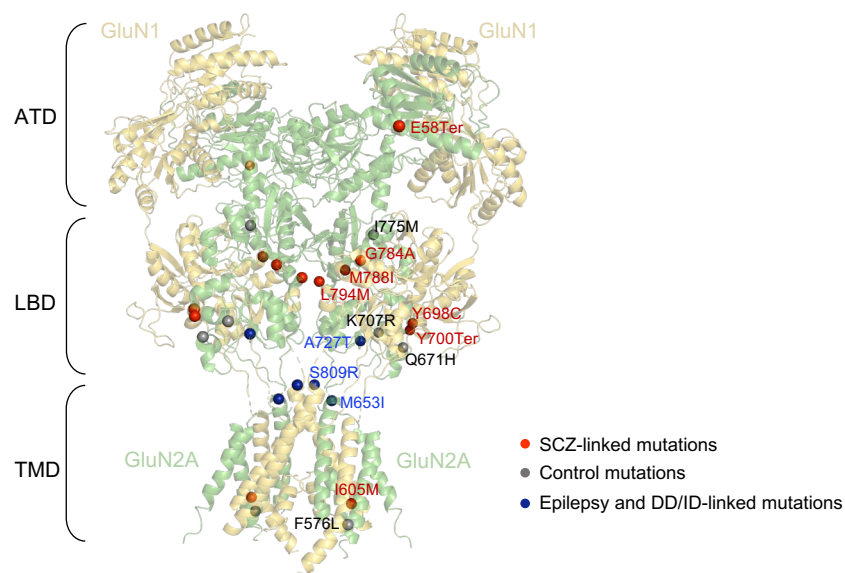


Figure S1. *GRIN2A* mutations mapped on human NMDAR structure. Protein structure of human NMDAR (PDB ID 6IRH) with two GluN1 (light yellow) and two GluN2A (light green) subunits. *GRIN2A* mutations associated with SCZ (red) or epilepsy/DD/ID (blue) as well as control mutations (dark gray) are mapped on the two GluN2A subunits of human NMDAR. Two SCZ-associated missense mutations (Q811P, G591R), one control mutation (R586K), one DD/ID-linked mutation (L812M) as well as mutations within the CTD were not mapped due to no structure coverage.

Figure S2

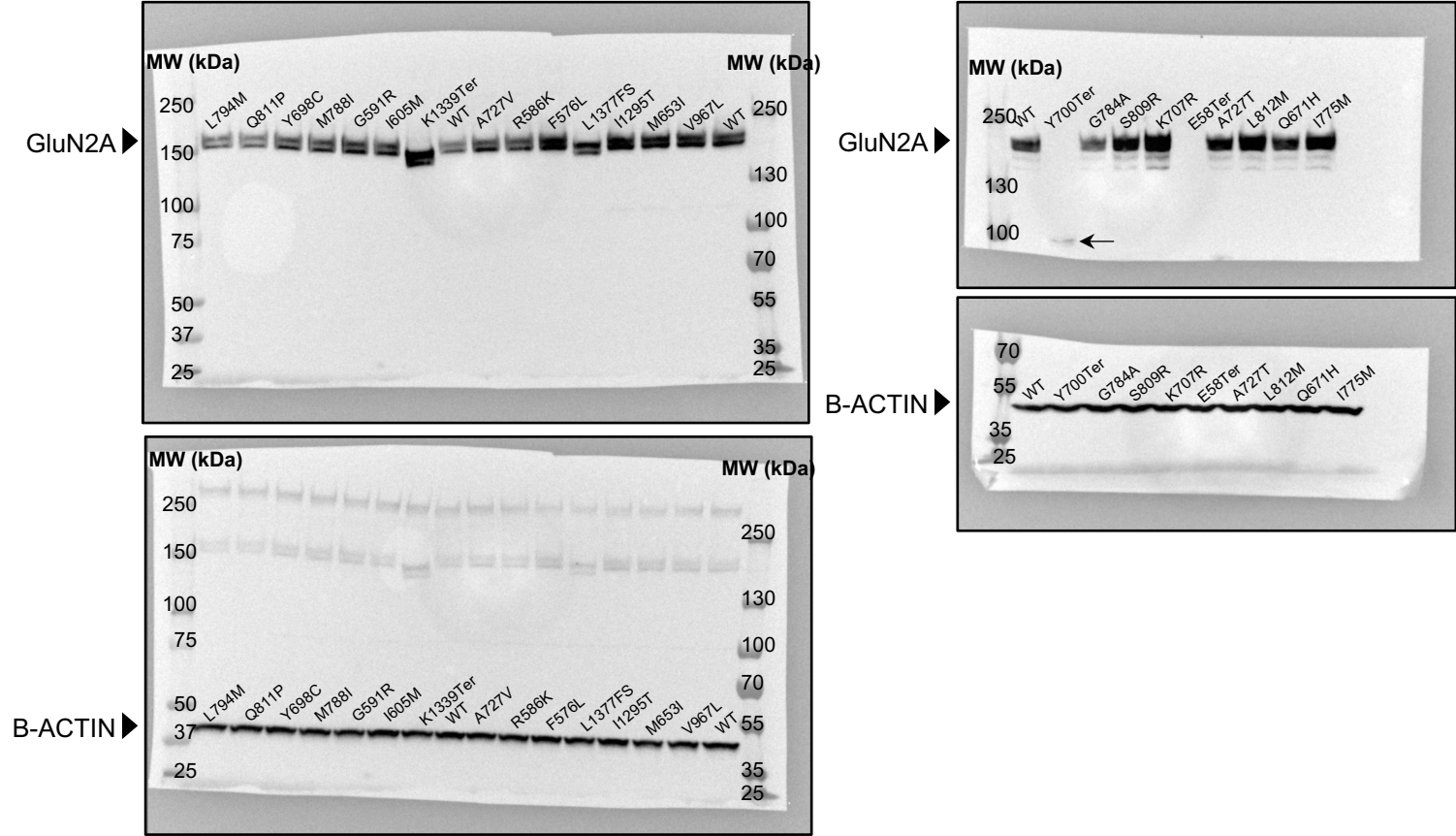


Figure S2. Uncropped western blot images of GluN2A variants. Western blots probing for GluN2A and β -ACTIN in lysates of HEK cells transiently transfected with GRIN1-GRIN2A constructs to express wild-type or mutant NMDARs. The arrow in Y700Ter lane indicates a faint band near the expected size for the Y700Ter fragment (~ 80 kDa).

Figure S3

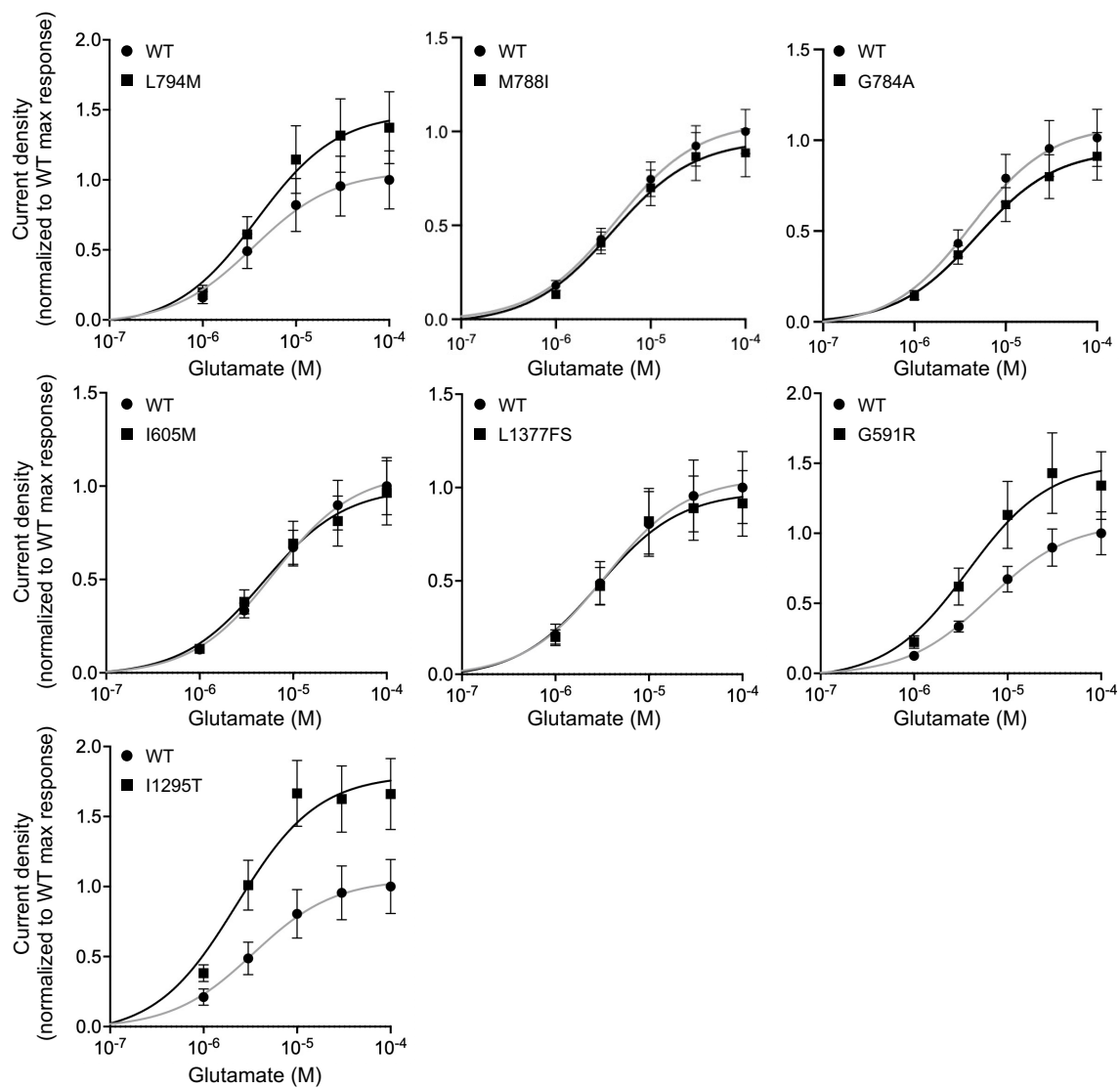


Figure S3. Effect of SCZ-associated *GRIN2A* variants on NMDAR function. Averaged current density in response to increasing concentrations of glutamate in the constant presence of 30 μ M glycine, normalized to maximal response, for NMDARs containing the wild-type or SCZ-associated GluN2A variants. The lines indicate a nonlinear regression three-parameter fit to each dataset. Data are displayed as mean \pm SEM, n = 31-81; see Table 1 for number of cells recorded per variant.

Figure S4

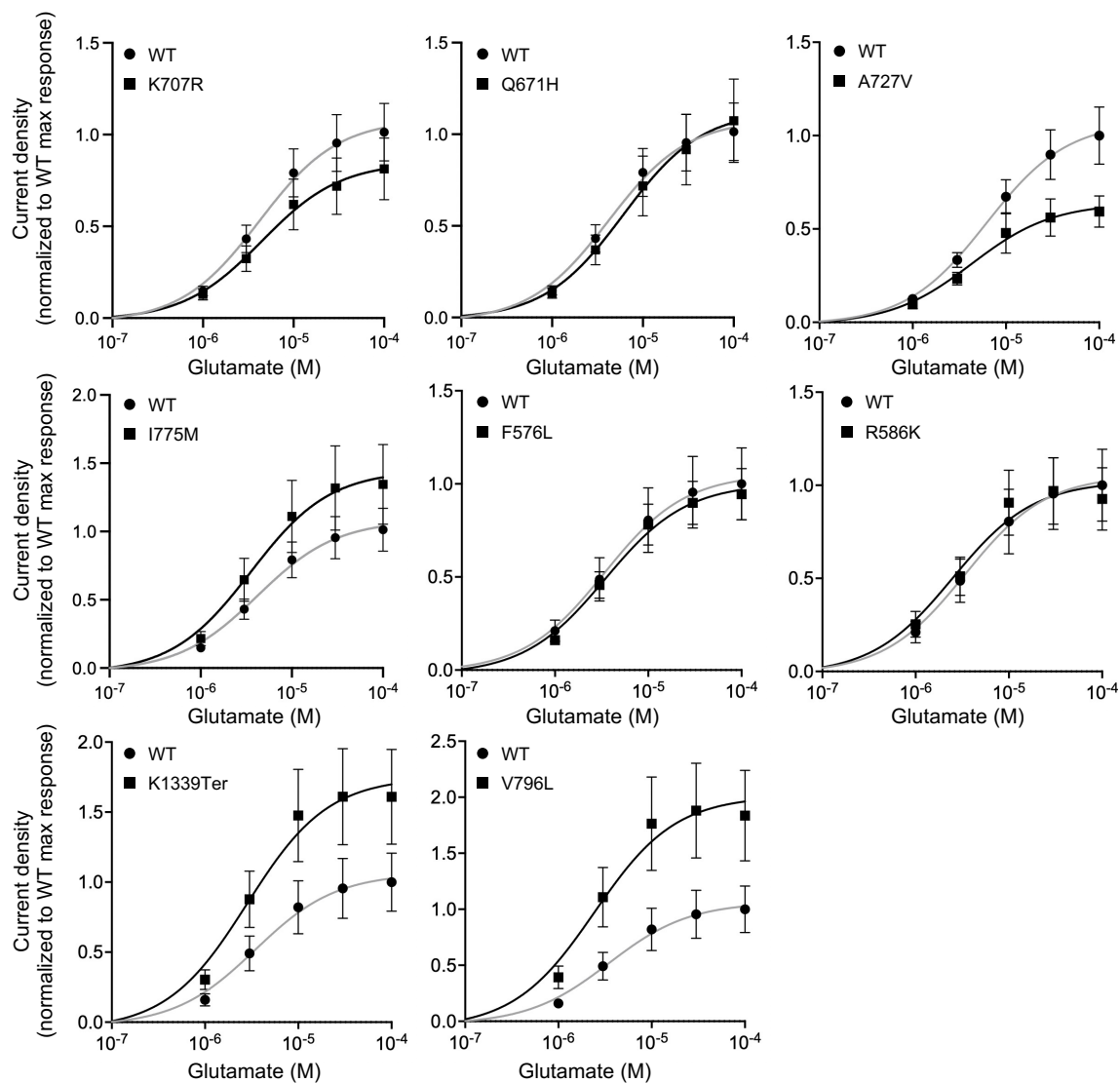


Figure S4. Effect of non-pathogenic *GRIN2A* variants on NMDAR function. Averaged current density in response to increasing concentrations of glutamate in the constant presence of 30 μ M glycine, normalized to maximal response, for NMDARs containing the wild-type or non-pathogenic GluN2A variants. The lines indicate a nonlinear regression three-parameter fit to each dataset. Data are displayed as mean \pm SEM, n = 17-70; see Table 1 for number of cells recorded per variant.

Figure S5

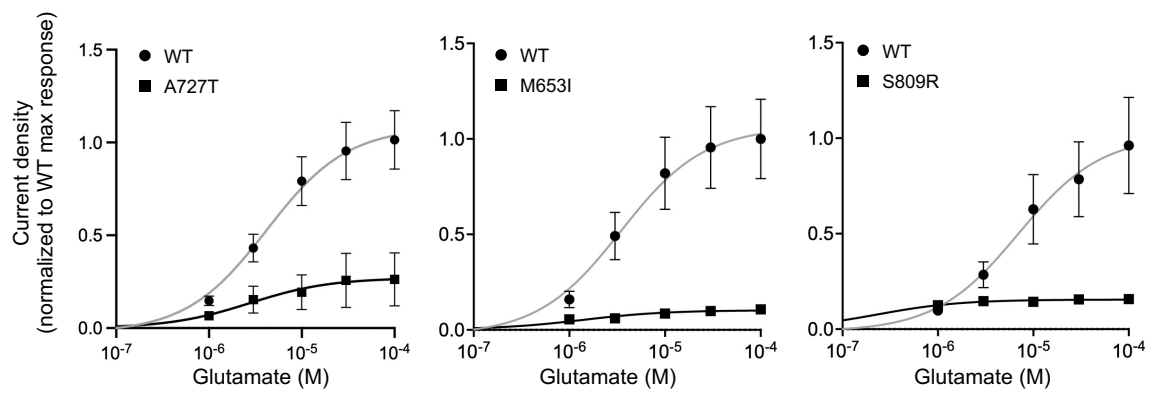


Figure S5. Effect of Epilepsy and DD/ID-associated *GRIN2A* variants on NMDAR function.

Averaged current density in response to increasing concentrations of glutamate in the constant presence of 30 μ M glycine, normalized to maximal response, for NMDARs containing the wild-type or Epilepsy and DD/ID-linked GluN2A variants. The lines indicate a nonlinear regression three-parameter fit to each dataset. Data are displayed as mean \pm SEM, n = 10-77; see Table 1 for number of cells recorded per variant.

Figure S6

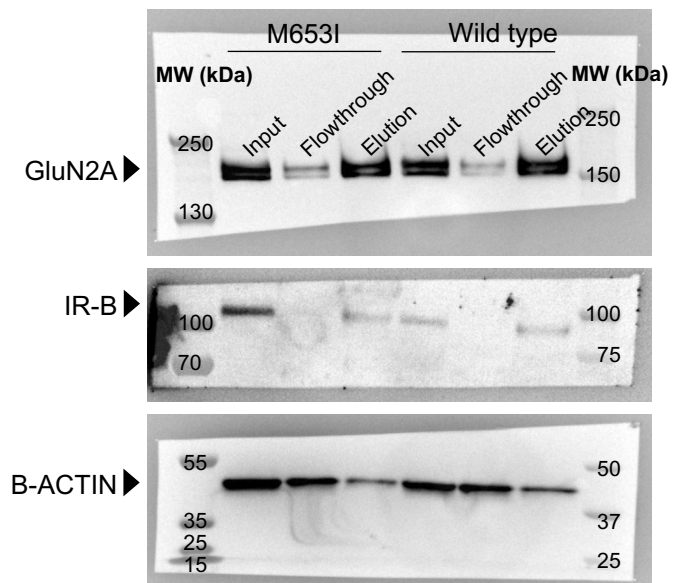


Figure S6. Original western blot images of the surface biotinylation experiment. Western blot probing for GluN2A, insulin receptor beta, and β -ACTIN in the input, flowthrough, and elution samples of surface biotinylation experiment done on HEK cells transiently transfected with *GRIN1-GRIN2A* constructs to express wild-type or M653I mutant NMDARs. Input, flowthrough, and elution represent total, internal, and surface expression respectively. IR-B: insulin receptor beta.